A Nonlinear Elastic Transmission for Variable-Stiffness-Actuation: Objective and Design

Soumen Sen, Antonio Bicchi

Abstract

Nonlinear elastic transmission is an essential component of mechanisms meant for passively variable stiffness. Variable-stiffness-actuation finds applications in areas like human friendly robots, legged machines, artificial prostheses, vibration control etc. Most of the designs in literature use nonlinearity in transmission for the sake of nonlinearity only − there does not exist any guideline for choosing the function. In this article, design of an elastic transmission is presented with an objective and a functional specification for an optimal stiffness behaviour. A principle is derived from passive properties of biological muscles to obtain the elastic function. Consequently, a general method is explained to synthesize a cam profile for the obtained function, followed by description of the spring design. Finally, an antagonistic implementation is presented with initial result.

Keywords: Nonlinear elastic transmission, Exponential spring, Variable-Stiffness-Actuation, Antagonistic actuation

1 Introduction

Impedance control has been put through for robotic manipulation in interactive tasks by Neville Hogan in [1]. However, impedance variability in everyday task ever prevail in the biological world. This forms an important area in contemporary biomechanics research [2]. In physical Human Robot Interaction (pHRI) impedance/stiffness variability has been proved to be effective in adding intrinsic safety [3], as well as in performance enhancement. Variable stiffness mechanisms have been successfully incorporated in applications such as legged locomotion [4], exoskeletons and rehabilitation devices [5], in structural vibration suppression [6], and automotive suspension system. One important attribute is that variability is achieved *passively* with an elastic element, where the transmitted force bears a *Nonlinear* relationship with the deflection the element undergoes. Till date, most of the designs of nonlinear springs have been done quite arbitrarily - nonlinearity for the sake of having a nonlinearity only. In such designs either a nonlinear elastically deformable material (e.g. rubber) has been used, or, a mechanism through mechanical linkages/cam with a *linear* spring has been built [7, 8]. In some designs nonlinearity of an abrupt change may be manifested near *singular* configurations.

In this article, a new nonlinear transmission design and its method are described, addressing some of the limitations stated above. One of the objectives is that the

Soumen Sen (Corresponding author)
Robotics and Automation, CMERI, Durgapur 713209, India, E-mail:soumen.sen@ieee.org.

Antonio Bicchi
Interdepartmental Research Centre “E. Piaggio”, University of Pisa, 56126 Pisa, Italy,
E-mail:bicchi@centropiaggio.unipi.it.

stiffness change should occur rapidly. To achieve an optimal stiffness behaviour, a *principle* is derived from properties of biological muscle following a model from literature [9] and a force-deflection *functional specification* is obtained in order to attain the optimal behaviour. Then, a general method is depicted to synthesize a cam profile and the mechanical design is presented. As example, an antagonistic implementation of variable stiffness actuation using the developed transmission is presented.

2 Nonlinear Elasticity of Transmission

2.1 Borrowing principle from biological muscle properties

It is not clear that which *force-displacement* function behaves best in varying stiffness. Apparently, this function should be task dependent, but there is no specific guideline hitherto available in literature. Stiffness/impedance variation is ubiquitous in nature and the living world does this in an efficient way. Hence, borrowing principle from biological muscle properties may help.

2.1.1 The principle

In search for the principle, we may study mathematical models of biological muscles from literature. Many of the researches on "*muscle*" are still based on A.V. Hill's model and subsequent refinements by A.F. Huxley [10, 11], which were based on very extensive and illustrious experiments. Later, Pinto and Fung in [9] have elaborately enlightened the solid-mechanics of muscle. Experiments show, a passive muscle fibre gets progressively stiffer with larger stretches. Pinto and Fung [9] has found that derivative of muscle *stress* (say s) with respect to *Lagrangian strain* (say ϵ_L) is linearly related to stress s at that point (the experiments were carried out on a rabbit heart muscle). It is established later that many collageneous tissues, including tendon, skin and skeletal muscle obey similar stress-strain characteristics. In notation,

$$\frac{ds}{d\epsilon_L} = \alpha(s + \beta),$$

where $\epsilon_L = \frac{L}{L_0}$, L_0 = initial length, L the current length and α and β are constant parameters.

Assuming the transmission body as a constant cross section length element, we can derive

$$\frac{L_0}{A}\frac{dF}{dx} = \alpha\left(\frac{F}{A} + \beta\right), \tag{1}$$

where, F is the force transmitted, A the invariant cross sectional area and x is the elongation. Above definition is equivalent to stating following proposition.

Proposition: The linear relationship between *stiffness* at a point of displacement and the *force* at that point leads to an *exponential* force-displacement characteristic,

$$F = \Phi(x) \;=\; \mu \exp\left(\frac{\alpha}{L_0}x\right) \;-\; K\,, \tag{2}$$

where, μ and $K = A\beta$ are constant coefficients and α is an exponent.

Proof: Integrating Eq. (1) we get the above expression in Eq. (2) as solution. x being the only independent variable, stiffness by definition is $\frac{\partial F}{\partial x} = \frac{\alpha}{L_0}(F + A\beta)$, which establishes the affine connection between stiffness and force. $\square$

2.1.2 Relative force error

Salisbury [12] had introduced the idea of designing a spring, based on the criterion of keeping the relative force error constant over the entire range of operation, $x > 0$. If $F = \Phi(x)$ be the force function, the relative force error can be expressed as $\frac{\delta F}{F} = \frac{1}{\Phi(x)} \frac{d\Phi(x)}{dx} \delta x$. Identifying a minimum sensible initial deflection of spring as δ_0 and the relative force error corresponding to δ_0 as C_0, then, if it is intended to maintain the relative error constant, above equation gives an exponential solution,

$$F = \Phi(x) = A \exp\left(\frac{C_0}{\delta_0} x\right). \tag{3}$$

Similarly, the relative force error, at $x = 0$ of Eq. (2) is $\frac{\delta F}{F} = \frac{\frac{\alpha}{L_0}\mu}{\mu - K}\delta_0$. It is interesting to note that the relative force error of Eq. (2) approaches a constant value over the range of operation $0 \le x \le X_{max}$ (maximum deflection), as illustrated in Fig. (1, right). A chosen value of $\alpha = \frac{C_0 L_0}{\delta_0}$ reduces the element into a Salisbury's spring.

Now, $K = \mu$ at $x = 0$ makes initial relative force error undefined. For other values of K, there will be a force offset, which is equivalent to a stiffness offset, because of the linearity in our chosen principle. In practice, the force offset (F_{min}) will never be zero and the minimum controllable force is limited by deadband (backlash), dry friction and motor torque ripple.

2.2 Synthesis of force-displacement function

For given δ_0 and C_0, the relative force error of Eq. (2) at L_0 is

$$\left.\frac{\delta F}{F}\right|_{L_0} = \frac{\mu \frac{\alpha}{L_0} \exp(\alpha)\ \delta_0}{\mu \exp(\alpha) - K} = C_0. \tag{4}$$

If F_{max} be the maximum force to be transmitted, then, defining dimensionless ratios, $F_{ratio} = \frac{F_{max}}{F_{min}}$, $L_{ratio} = \frac{X_{max}}{L_0}$, and $S_{ratio} = \frac{C_0 L_0}{\delta_0}$, the following nonlinear equation needs to be solved to determine exponent α,

$$\alpha \exp(\alpha)\ (F_{ratio} - 1) + S_{ratio} \exp(\alpha) - S_{ratio} \exp(L_{ratio}\alpha) = 0. \tag{5}$$

which is obtained after some reduction and eliminations using the expressions, $K = F_{min}\left(\frac{S_{ratio}}{\alpha} - 1\right)$ and $\mu = \frac{F_{max}+K}{\exp(\alpha L_{ratio})}$. K and μ are obtained easily using other boundary conditions involving $F_{max},\ F_{min}$, and X_{max}.

For the chosen specification of $L_0 = 5mm$, $F_{max} = 100N$, $F_{min} = 0.5N$, $X_{max} = 50mm$, $C_0 = 0.01N/N$ and $\delta_0 = 0.1mm$, value of $\alpha = 0.61$ is computed from Eq. (5) and following is obtained as a reasonable spring,

$$F = 0.224 \exp(0.122x) + 0.09, \tag{6}$$

Fig. (1, left) shows force behaviour with deflection for both the designed and the actual spring .

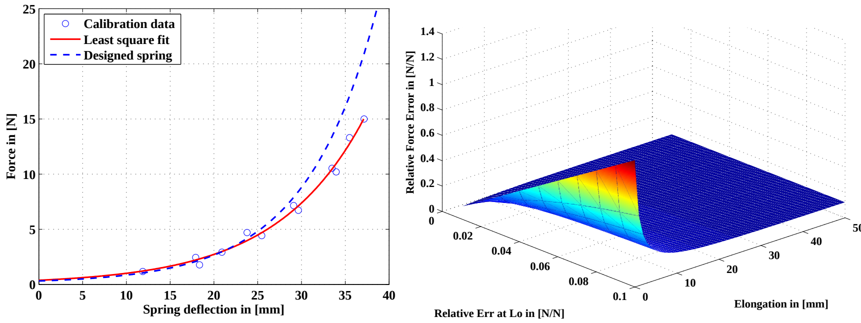

Figure 1: (Left) The exponential spring of Eq. (6) designed from first principle. Specification given by $L_0 = 5mm$, $F_{max} = 100N$, $F_{min} = 0.5N$, $X_{max} = 50mm$, $C_0 = 0.01N/N$, $\delta_0 = 0.1mm$ and exponent $\alpha = 0.61$. This figure also superimposes calibration data of the actually developed physical spring in section 3.2. The deviations are due to nonzero roller radius, friction and manufacturing error of the cam profile, discussed in the next section. The spring actually can elongate till 50mm. (Right) Relative force error with displacement, as the initial force error is varied for the above designed spring.

2.3 Performance comparison among a class of spring functions

It is imperative that how fast a particular stiffness mechanism can adapt the demand of stiffness change depend on the passive force-displacement characteristic inherent in the elastic element. Here, an attempt is made to understand the *mechanics* in view of this rapidity. The basic simple model used for benchmarking the examination is shown in Fig. (2, left). This resembles the famous *Brachistochrone* problem of Johann Bernoulli, but we don't have any unique analytical solution similar to the *Brachistochrone Cycloid*. Intuitively, the fastest motion can occur if all the *potential energy* stored can be transformed into kinetic energy instantly from rest; a step function arises (which is discontinuous), i.e. *stiffness* should fall in a step. However, present requirement is for a continuous function in view of realizability.

We restrict our view within functions leading to periodic oscillations, namely, power springs of the form $\Psi(x) = ax^n$, where, a is a constant coefficient and n is an integer exponent. Fractional exponents $0 < n < 1$ are not considered. These are conservative systems of the form $\ddot{x} + \Psi(x) = 0$. Multiplying by $\dot{x}$, an integral equation is obtained

$$\frac{1}{2}\dot{x}^2 + \int_0^x \Psi(\eta)d\eta = \text{constant} = \text{Total energy}. \tag{7}$$

The second term is the potential energy and is given by $\int_0^x \Psi(\eta)d\eta = \frac{ax^{n+1}}{n+1}$. We study (rather in a brute force way) rapidness behaviours of these basic functions. As shown in Fig. (2, left), numerically free motion of the spring mass system is solved with U_0 at rest. U_0 is kept equal for all, as well the stiffness value ($K_0 = \frac{\partial^2 U}{\partial x^2}\Big|_{x=x_0}$).

Minimum time behaviours of motion between two stiffness values K_0 and K_f for all springs are watched.

Simulation results are shown in Fig. (2, right). A trend is observed that the power springs tend to reach a minimum time value with increasing integer exponent n. It is compared with an exponential function of the form $\Psi(x) = sign(x) a \exp(b\,|x|)$; with the specified K_0 and K_f, it is seen to operate in a minimum time among all the springs dealt here. However, this function does not have an equilibrium point, but is stable about origin. For this spring, x_0 is chosen corresponding to a linear spring for given U_0 and K_0. Final position is computed by $x_f = \frac{1}{b} \log\left(\frac{K_f}{ab}\right)$. Simulations show that an exponential spring can act fastest in moving from K_0 to K_f(see caption of Fig. (2)).

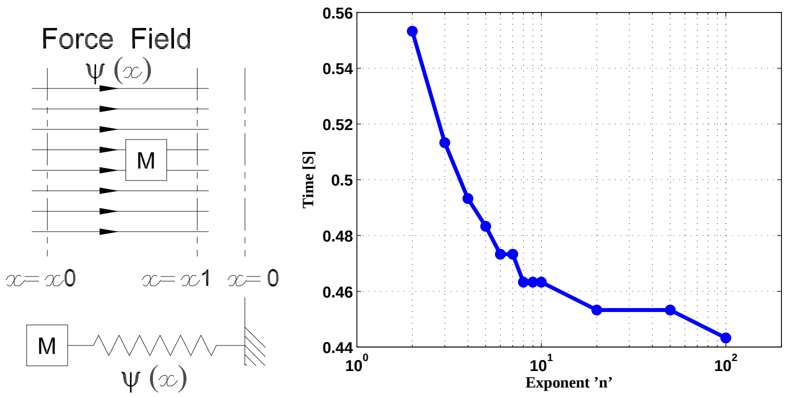

Figure 2: (Left) A mass M is acted on under a *central conservative* force field (top). Equivalent spring-mass system is in the bottom. (Right) Mass, $M = 0.1kg$, initial stored energy is $U_0 = 0.1J$ and the initial deflection $x = 100mm$ for all the springs. The system is released from rest with U_0 and the time to reach from stiffness values K_0 to $K_f = K_0/2$ is observed. Power springs show decreasing time with increasing n. The behaviour tends to reach a minimum time as $n \to \infty$. For a chosen *exponential* spring, the movement from stiffness K_0 to K_f happens with a *minimum time* of $0.44S$ which is lowest among all the springs considered. The dynamics is solved numerically using variable order, multistep solver (namely ode15s of Matlab©).

3 Design for Any Continuous Monotonic Function

Several designs of nonlinear springs are available in literature, including variable cross section leaf spring, conical spring, Belleville spring, linear-spring-linkage mechanisms and even exploiting nonlinear properties of rubber etc. None of these is suitable for attaining a specified function. Migliore et al. in [13] developed a quadratic spring using cam profile. The present design looks similar to this, but carries a fundamental difference which has been developed independently and is more methodical. The approach of this article exploits *virtual work* principle (unlike the method in [13]), which is elegant, more general and analytical and suitable for realizing any arbitrary continuous monotonic spring function.

3.1 Synthesis of cam profile

One way to physically realize a desired function is incorporating a cam profile with a follower loaded by a linear spring. Synthesis of such a profile needs a transformation from the force-displacement domain in Eq. (2) to a cartesian geometric plane. Here, it is achieved using *principle of virtual work*. This is a general method in the sense that any continuous monotonic function can be realized in a physical design.

Say, $Y = \Psi(x)$ is the desired cam profile, where Y is the displacement of the cam follower, which is loaded by a linear spring of fixed stiffness k_s. Desired force function in cartesian X is $F_X = F$ of Eq. (2). Fig. (3, left) explains the principle (one half of the mechanism). With a co-efficient of rolling friction ν, $F_X = F_S \frac{\nu+\tan\theta}{1-\nu\tan\theta}$, where, F_S is a function of position Y.

In order to arrive at an initial solution, we simplify the problem by assuming the following: rolling friction is zero and the roller radius is small enough so that the locus of the roller centre and the geometric profile $Y = \Psi(x)$ is indistinguishable. For virtual displacements of Δx and Δy, virtual work equality is given by

$$2\,k_s\,Y dy \;=\; F_X\,dx, \quad \text{where 2 accounts for two sides of the profile.}$$

Using expression for F_X and solving above differential equation, we get

$$\Psi(x) \;=\; \sqrt{\frac{1}{k_s}\left\{\frac{\mu L_0}{\alpha}\exp\left(\frac{\alpha}{L_0}x\right) \;-\; K\,x \;+\; C\right\}}, \tag{8}$$

where, C is constant of integration. With zero initial condition, $C = -\frac{\mu L_0}{\alpha}$.

3.2 Physical realization

The synthesized cam profile is reproduced in an Aluminium block by CNC milling. A 'V' groove along the profile guides the follower wheel. Follower wheel is spring loaded with constant $k_s = 1N/mm$ approximately. The wheel and the spring again are mounted on another carriage,which is pulled by a rod. The stiffness is actually felt at this rod end. A CAD model is illustrated in Fig. (3, right). The actual assembled spring can be seen in the photograph of experimental set up shown in Fig. (4).

The spring is calibrated by measuring the displacement through an encoder mounted on a pulley. Force is measured in steady states along a pulling rope , attached on the rod end by a digital linear force gauge of $0.1N$ resolution obtained from Mecmesin. A nonlinear least-square fit characteristic $F = 0.368\exp(0.099x) + 0.01$ is obtained, which is plotted in Fig. (1, left), along with the measured data points.

4 Implementation: A Simple Antagonistic Experimental Setup

Variable stiffness actuation can be implemented in various ways and be broadly divided into (1) mechanisms for explicit stiffness control and (2) stiffness control through antagonistic actuation. In type-2, stiffness generating forces belong to the kernel of the

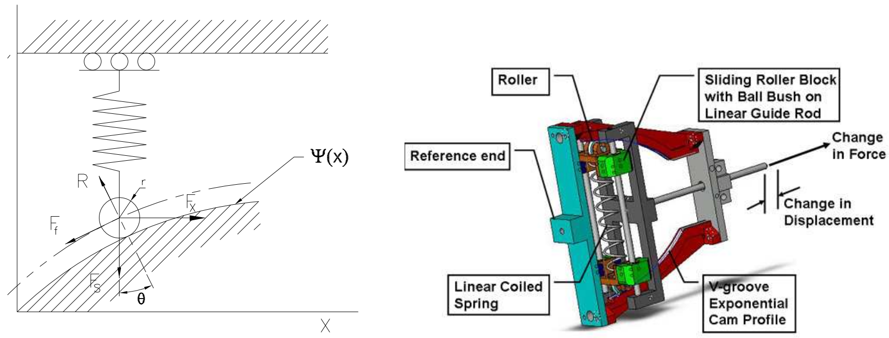

Figure 3: (Left) Virtual work principle is applied to synthesize the geometric profile $\Psi(x)$. F_S is the linear-spring force, F_f is friction-force, R is the reaction, θ is the instantaneous contact angle. r be the roller radius. (Right) CAD model of the designed exponential spring.

input forces resembling a two-fingered grasp. This antagonistic actuation prevail musculoskeletal system of the animal world. In the present setup, a robot joint is driven by two motors in antagonism through tendons on exponential elastic transmission elements as developed above. This setup, as illustrated in Fig. (4, left), is primarily meant for carrying out experiments to validate different controller algorithms for simultaneous control of motion and stiffness. One such algorithm uses tendon-force-sensors to implement a *null-spacel force based impedance controller*. Fig. (4, right) shows one such result, where, joint velocity and stiffness vary inversely. As stated earlier, stiffness is related to the null-space (internal) forces of the tendon system through a linear relationship because of exponential characteristic. Internal force in the figure is proportional to joint stiffness (in absence of external load).

5 Conclusions

The article has described development of a nonlinear elastic transmission element whose design is motivated from the properties of biological muscle. First an objective is identified in terms of rapidity of change in stiffness. Then, a principle is derived from muscle fibre passive property that stiffness should be proportional to force, which leads to an exponential characteristic. Simulations are carried out to examine and compare the rapidity of stiffness variation behaviour among a class of power springs and exponential spring. It is observed that an exponential spring can behave faster than the others in the class. An exponential spring is then designed from a given specification. A *virtual work principle* based method is adopted for synthesizing a *cam profile*, unlike the development in [13]. This method is analytical and general and can be used for any arbitrary continuous monotonic function. The spring components are manufactured and assembled and the final spring is then calibrated to find its characteristic and is compared with the original designed function. Small deviation of the actual characteristic from the designed one is likely to be due to presence of friction, zero roller diameter assumption and manufacturing error of the profile. Finally, one experimental antagonistic implementation is described using two such exponential springs, driven

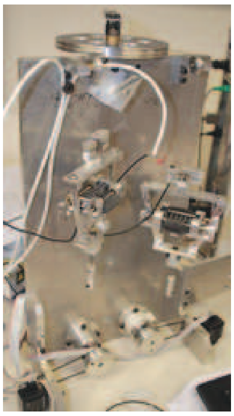

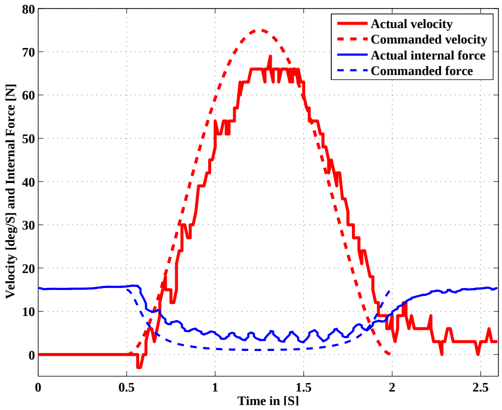

Figure 4: (Left) Simple antagonistic Variable Stiffness Actuator. (Right) The joint is commanded to move following a quintic trajectory through 60 deg in $1.54S$. Commanded joint velocity (V) and internal force (F_{int}) follows $F_{int} = \frac{F_{limit}}{1+10\|V\|}$, F_{limit} is a limit force. The velocity and stiffness responses are shown.

by motors and tendons. The setup is intended for carrying out experiments for test and validation of controller algorithms. One such *Null-space Force Based Impedance Controller* using force sensors is tested on this setup and initial result of simultaneous control for internal-force (stiffness) and motion is presented.

Acknowledgement

First author expresses his gratitude to Interdepartmental Research Centre "E. Piaggio", University of Pisa, Italy for providing scope, facilities and financial support for the development work in this report.

References

[1] N. Hogan, "Impedance control: an approach to manipulation, parts i, ii, iii," *Trans. of ASME, Journal of Dynamics, Systems, Measurement and Control*, vol. 107, 1985.

[2] E. Burdet, R. Osu, D. Franklin, T. Milner, and M. Kawato, "The central nervous system stabilizes unstable dynamics by learning optimal impedance," *Nature*, vol. 414, no. 6862, pp. 446–449, 2001.

[3] A. Bicchi and G. Tonietti, "Fast and soft arm tactics: Dealing with the safety–performance tradeoff in robot arms design and control," *IEEE Robotics and Automation Magazine*, vol. 11, Special issue on "Safety Among Us", June 2004.

[4] J. Hurst, J. Chestnutt, and A. Rizzi, "An actuator with physically variable stiffness for highly dynamic legged locomotion," in *IEEE International Conference on Robotics and Automation*, (New Orleans), 2004.

[5] M. Cherry, D. Choi, K. Deng, S. Kota, and D. Ferris, "Design and fabrication of an elastic knee orthosis - preliminary results," in *ASME IDETC/CIE*, (Philadelphia), 2006.

[6] J. Leavitt, F. Jabbari, and J. Bobrow, "Optimal control and performance of variable stiffness devices for structural control," in *American Control Conference*, (Portland), pp. 2499–2504, 2005.

[7] R. Schiavi, G. Grioli, S. Sen, and A. Bicchi, "Vsa-ii: a novel prototype of variable stiffness actuator for safe and performing robots interacting with human," in *IEEE International Conference on Robotics and Automation*, (Pasadena), 2008.

[8] S. Wolf and G. Hirzinger, "A new variable stiffness design: Matching requirements of the next robot generation," in *IEEE International Conference on Robotics and Automation*, (Pasadena), 2008.

[9] J. Pinto and Y. Fung, "Mechanical properties of the heart muscle in the passive state," *Journal of Biomechanics*, vol. 6, 1973.

[10] A. Huxley, "Muscle structure and theories of contraction," *Prog. Biophys. Chem.*, vol. 7, 1957.

[11] T. McMahon, *Muscles, Reflexes, and Locomotion*. Princeton, NJ,: Princeton University Press, 1984.

[12] T. Mason and K. Salisbury, *Robot Hands and the Mechanics of Manipulation*. Cambridge, MA: MIT Press, 1985.

[13] S. Migliore, E. Brown, and S. DeWeerth, "Biologically inspired joint stiffness control," in *IEEE International Conference on Robotics and Automation*, (Barcelona), April 2005.